Structure, Chemical Bonding, and Nuclear Quadrupole Interactions of β-$Cd(OH)_2$: Experiment and First Principles Calculations

L. Hemmingsen,*,† R. Bauer,† and M. J. Bjerrum‡

Department of Mathematics and Physics and Department of Chemistry, The Royal Veterinary and Agricultural University, Thorvaldsensvej 40, DK-1871 Frederiksberg C, Denmark

K. Schwarz and P. Blaha

Institut für Technische Electrochemie, Technische Universität Wien, A-1060 Vienna, Austria

P. Andersen

Department of Chemistry, University of Copenhagen, Universitetsparken 5, DK-2100 Copenhagen Ø, Denmark

Received January 6, 1999; Revised Manuscript Received April 11, 1999

The structure of $Cd(OH)_2$ was determined by X-ray diffraction on powder crystals and by calculations using the full-potential linearized augmented plane wave method. Good agreement between the two results was found. The chemical bonding is characterized by the interactions of the OH^- group with Cd^{2+} which is not only electrostatic but shows some polarization or covalent admixtures and by the covalent bond in the OH^- group. The electric field gradient (EFG) was calculated and compared with an experimental determination of the nuclear quadrupole interaction using perturbed angular correlation of γ-rays. The calculated EFG agrees well with the EFG derived from experiment. The total electric field gradient was decomposed into contributions from different orbitals and energy regions showing that both the Cd 5p and 4d wave functions contribute significantly. Finally, the influence of spin-orbit coupling on the electric field gradient was investigated and found to be of little importance.

Introduction

The structure of $Cd(OH)_2$ is shown in Figure 1 and belongs to a large class of layered structures that can be described as a more or less perfect packing of larger anions with smaller cations lying in the intersticies of the packing.

The unit cell is hexagonal and contains a single molecule. The atoms are in the following special positions of $P\bar{3}ml$ (D^3_{3d}, Int. Tab. No. 164):

Cd	(1a)	0,	0,	0;			
O	(2d)	$^1/_3$,	$^2/_3$,	z(O);	$^2/_3$,	$^1/_3$,	$-z$(O)
H	(2d)	$^1/_3$,	$^2/_3$,	z(H);	$^2/_3$,	$^1/_3$,	$-z$(H)

That is, there are only two atomic coordinates to be optimized in a structure determination (z(O) and z(H)). The structure of $Cd(OH)_2$ has been studied previously by X-ray diffraction[1,2] in which the unit cell parameters and the position of the oxygen atom, but not of the hydrogen atom, were determined. The standard approach to determine the position of the hydrogen nucleus is to apply neutron scattering, but since naturally occurring cadmium has a very large cross-section for neutron absorption, this is not feasible for $Cd(OH)_2$. Therefore a combination of X-ray diffraction and calculations is applied in this work.

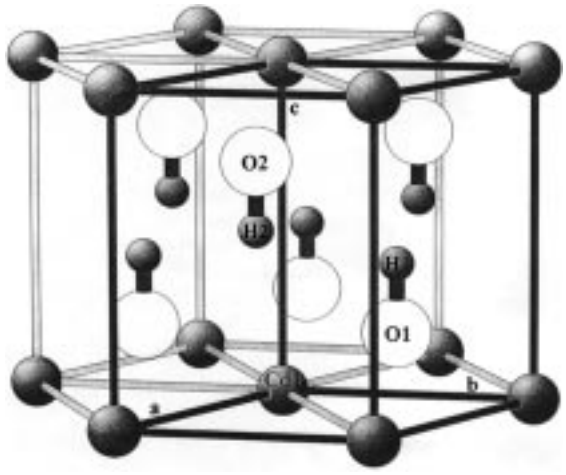

Figure 1. Cadmium coordination geometry and the unit cell of β-$Cd(OH)_2$. The coordinate system to which the LAPW calculations refer is centered at Cd1 with the z axis along c, the y axis along b, and consequently the x axis bisecting the angle between the two cadmium ions closest to the reader (in the lower plane of cadium ions).

Several investigations, based on density functional theory (DFT), have been performed with the full-potential linearized augmented plane wave (LAPW) method, mostly on known structures of crystalline systems. The corresponding electric field gradients (EFGs) have in several cases been calculated, too,

* Corresponding author.
† Department of Mathematics and Physics, RVAU.
‡ Department of Chemistry, RVAU.

(1) Glasser, L. S. D.; Roy, R. *J. Inorg. Nucl. Chem.* **1961**, *17*, 98.
(2) Bertrand, G.; Dusausoy, Y. *C. R. Acad. Sc., Ser. C* **1970**, *270*, 612.

10.1021/ic990018e CCC: $18.00
Published on Web 05/26/1999

and they agree on average within 10−20% with experimental data.[3−9]

Perturbed angular correlation of γ-rays (PAC) experiments have been applied extensively to determine nuclear quadrupole interactions (NQI). Most studies have been performed on the crystalline state,[10] but in recent years a substantial effort has been devoted to measurements on metal ion containing proteins in solution.[11−15] In this context cadmium is used as a substitute for zinc in zinc-containing enzymes to allow ^{111m}Cd PAC and ^{113}Cd NMR spectroscopy. In such enzymes it is often assumed that OH^- is coordinating to the metal ion as a nonprotein ligand. Therefore it is important to understand the bonding and the origin of the NQI in OH^- containing cadmium complexes. $Cd(OH)_2$ is interesting because it is a simple system which can play the role as a representative test case that can provide fundamental insight concerning the bonding properties of cadmium complexes.

In this work we combine the X-ray, PAC, and LAPW techniques to study the structure, chemical bonding, and EFG of $Cd(OH)_2$. $Cd(OH)_2$ is a system well suited for first principles calculations on a cadmium complex because of the relatively small number of electrons in the unit cell. Furthermore, due to the simple structure, it is possible to determine the molecular structure by X-ray diffraction on a powder crystalline sample. Finally, since there is only one well-defined metal site, it is straightforward to fit and interpret the PAC spectrum.

Experimental Section

$Cd(OH)_2$ Sample Preparation. Small crystals of $Cd(OH)_2$ for powder X-ray analysis were obtained from aqueous solution by dropwise mixing of 1.9 g (0.048 mol) of NaOH in 60 mL of water with 6.2 g (0.02 mol) of $Cd(NO_3)_2{\cdot}4H_2O$ in 60 mL of water, which was kept carbondioxide free in the whole preparation. Crystals of $Cd(OH)_2$ are immediately formed. The precipitated crystals were separated from the supernatant by centrifugation and washed several times with water and finally dried in a vacuum exsiccator at room temperature. Crystals of $Cd(OH)_2$ doped with $^{111m}Cd^{2+}$ were prepared in smaller quantities for the PAC experiment by dropwise adding a solution of 0.16 g (0.004 mol) of NaOH in 5 mL of water to a solution of 0.5 g (0.0016 mol) of $Cd(NO_3)_2{\cdot}4H_2O$ in 5 mL of water to which a small amount of radioactive $^{111m}Cd^{2+}$ was also added. The precipitated crystals were seperated from the supernatant by centrifugation, washed several times with water, and partially air-dried. The moist crystals were directly used in the PAC experiment.

X-ray Powder Diffraction and Structure Determination. A Stoe Stadi P X-ray powder diffractometer was used to obtain diffraction data at 21 °C from freshly prepared samples of small crystals of $Cd(OH)_2$ in 0.3 mm capillaries. The radiation was Cu $K\alpha_1$ selected by a curved germanium monochromator. Data were collected in the 2Θ range 15−92° in 0.01° intervals using a position-sensitive detector covering 7° in 2Θ. The software Visual X^{POW} (1995) and CSD (Crystal Structure Determination, Version 4.1, 1994) supplied with the instrument was used for the initial data treatment and the final Rietveld analysis, respectively, including the atomic scattering factors for Cd, O, and H given in CSD.

PAC Experiments. ^{111m}Cd was produced by irradiating a ^{108}Pd target on a small graphite block with 21 MeV α-particles for 1.5 h in a beam of about 30 μA. This gave an activity of about 400 MBq at the time the cyclotron was stopped. A detailed description of the preparation of the target and of the extraction of ^{111m}Cd after irradiation can be found in Hemmingsen et al.[11] The irradiation was performed at the Cyclotron Department of the University Hospital in Copenhagen.

The experimental setup is a build out version of the PAC camera described elsewhere.[16] It consists of 6 detectors, each pointing toward one face of an imaginary cube, at the center of which the sample is positioned. It has a facility which continously maintains the optimal source−detector distance (depending on the activity of the source) and a Peltier element for controlling the temperature in the range −10 to 40 °C. The time resolution is 0.850 ns.

The PAC measurements were performed at 274 K on samples (100−200 mg) of randomly oriented small crystals (kept in plastic tubes) of $Cd(OH)_2$ doped with $^{111m}Cd^{2+}$.

Fitting to PAC Spectra. The theory of PAC for a sample of identical, static and randomly oriented molecules is briefly described here, while a thorough presentation can be found in Frauenfelder and Steffen.[17]

PAC measurements require an isotope which decays by the succesive emission of two γ-rays. For example ^{111m}Cd has this property and the important point is, that the two γ-rays are not emitted in random directions with respect to each other, i.e., there is an angular correlation between them. The correlation will depend on properties of the nuclear decay and on the nuclear quadrupole interaction, i.e., the electric interaction between the nuclear quadrupole moment and the EFG from the surrounding charge distribution. In ^{111m}Cd PAC spectroscopy, the probability density of detecting the second γ-ray, γ_2, at an angle θ (with respect to the direction of γ_1) at time t after the first γ-ray, γ_1, is given by

$$P(\theta, t) \propto \exp(-t/\tau)(1 + A_2 G_2(t) P_2(\cos\theta)) \qquad (1)$$

where τ is the lifetime of the intermediate nuclear energy level, A_2 is a constant, $P_2(\cos\theta)$ is the Legendre polynomial of second order, and

$$G_2(t) = a_0 + \sum_{i=1}^{3} a_i \cos(\omega_i t) \qquad (2)$$

where the a_i and ω_i depend on the NQI, that is, $G_2(t)$ contains the information we wish to extract from an experiment.

In the experimental setup the six detectors monitor $P(\theta, t)$, for angles of 90 or 180° between the two γ-rays. The measured quantity is the number of γ_2 detections at time t after γ_1, $W(\theta, t)$, with θ equal to 90 or 180°. For each of these spectra the background due to accidental coincidences is subtracted and the zero point in time is adjusted using a ^{75}Se source. The latter also emits two consecutive γ-rays, but the lifetime of the intermediate level is very short, i.e., detection of the two γ-rays must be simultaneous.

Using eq 1 $A_2G_2(t)$ is determined experimentally as

$$A_2 G_2(t) = 2\frac{W(180°, t) - W(90°, t)}{W(180°, t) + 2W(90°, t)} \qquad (3)$$

where $W(180°, t)$ denotes the 6th root of the product of the six 180°

(3) Blaha, P.; Schwarz, K.; Herzig, P. *Phys. Rev. Lett.* **1985**, *54*, 1192.
(4) Schwarz, K.; Ambrosch-Draxl C.; Blaha P. *Phys. Rev.* **1990**, *B42*, 2051.
(5) Schwarz, K.; Blaha, P. *Z. Naturforsch.* **1992**, *47A*, 197.
(6) Blaha, P.; Singh, D. J.; Sorantin, P. I.; Schwarz, K. *Phys. Rev.* **1992**, *B46*, 1321.
(7) Dufek, P.; Blaha, P.; Schwarz, K. *Phys. Rev. Lett.* **1995**, *75*, 3545.
(8) Blaha, P.; Dufek, P.; Schwarz, K.; Haas, H. *Hyperfine Interactions* **1996**, *97*, 3.
(9) Winkler, B.; Blaha, P.; Schwarz, K. *Am. Miner.* **1996**, *81*, 545.
(10) Lerf, A.; Butz, T. *Hyperfine Int.* **1987**, *36*, 275.
(11) Hemmingsen, L.; Bauer, R.; Bjerrum, M. J.; Zeppezauer, M.; Adolph, H. W.; Formicka, G.; Cedergren-Zeppezauer, E. *Biochemistry* **1995**, *34*, 7145.
(12) Hemmingsen, L.; Bauer, R.; Bjerrum, M. J.; Adolph, H. W.; Zeppezauer, M.; Cedergren-Zeppezauer, E. *Eur. J. Biochem.* **1996**, *241*, 546.
(13) Danielsen, E.; Kroes, S. J.; Canters. G. W.; Bauer R.; Hemmingsen, L.; Singh, K.; Messerschmidt A. *Eur. J. Biochem.* **1997**, *250*, 249.
(14) Bauer, R.; Danielsen, E.; Hemmingsen, L.: Bjerrum, M. J.; Hansson, Ö.; Singh, K. *J. Am. Chem. Soc.* **1997**, *119*, 157.
(15) Bauer, R.; Danielsen, E.; Hemmingsen, L.: Sørensen, M. V.; Ulstrup, J.; Friis, E. P.; Auld, D. S.; Bjerrum, M. J. *Biochemistry* **1997**, *36*, 11514.
(16) Butz, T.; Saibene, S.; Fraenzke, T.; Weber, M. *Nucl. Instr. Methods Phys. Res., Sect. A* **1989**, *284*, 417.
(17) Frauenfelder, H.; Steffen, R. M. α-, *β- and γ-Ray Spectroscopy*; Siegbahn, K., Ed.; North-Holland: Amsterdam, 1965; Vol. 2, p 997.

spectra (after background subtraction and zero-point adjustment) and $W(90°, t)$ denotes the 24th root of the twentyfour 90° spectra.

The experimentally determined $A_2G_2(t)$ is fitted with the expression given in eq 2. The fitting parameters are ω_0 and η. The a_i and ω_i are functions of these two parameters, see for example Frauenfelder and Steffen[17] for a detailed presentation.

ω_0 is defined as

$$\omega_0 = \frac{3}{20\hbar}|eQV_{zz}| \tag{4}$$

where e is the unit charge, Q is the nuclear quadrupole moment of the ^{111}Cd nucleus in the intermediate ($I = {}^5/_2$) state, and V_{zz} is the principal component of the EFG tensor. ω_0 gives an indication of the strength of the interaction. The value of Q used in this work is 0.83(13) b.[18] η is the so-called asymmetry parameter defined as

$$\eta = \frac{V_{xx} - V_{yy}}{V_{zz}} \tag{5}$$

where V_{xx} and V_{yy} are the other two eigenvalues of the EFG tensor (chosen so that $|V_{xx}| \le |V_{yy}| \le |V_{zz}|$). The value of η is by definition between zero and one, where zero corresponds to an axially symmetric EFG tensor.

Density Functional Calculations. Energy band structure calculations have been performed using the full potential linearized augmented plane wave (LAPW) method as embodied in the WIEN97 code.[19,20] In this method the unit cell is decomposed into atomic spheres around the atoms (Cd, O, and H with radii of 1.8, 1.2, 0.6 au, respectively) and an interstitial region. Well-converged plane wave basis sets with $R_{min}K_{max} = 4.0$ and up to 40 k points in the irreducible wedge of the Brillouin zone were used. To improve upon the linearized basis set "local orbitals" for Cd 4p and O 2s states are added. The calculations are based on density functional theory and we used both, the local density approximation (LDA)[21] as well as the more advanced generalized gradient approximation (GGA) due to Perdew and Wang.[22] The lattice parameters a and c were taken from experiment (see Table 1), but the z(O) and z(H) positional parameters were optimized by total energy minimization using the forces acting on the nuclei as an additional criterion for the minimization.[23]

Spin−orbit coupling was added to the scalar−relativistic calculations (including mass−velocity and Darwin terms) in a second variational step, in order to test the influence on the EFG.

The density of states (DOS) was calculated using a modified tetrahedron method[20] and weighted using partial charges within the respective atomic spheres.

The EFG on all atomic sites was calculated directly from the selfconsistent total charge density $\rho(\mathbf{r})$ of the crystal without any adjustable parameters using[3−5]

$$V_{zz} = \int \frac{\rho(\mathbf{r})Y_{20}(\hat{\mathbf{r}})}{r^3} d\mathbf{r} \tag{6}$$

where $Y_{20}(\hat{\mathbf{r}})$ is the usual spherical harmonic (appropriately normalized). The EFG can easily be decomposed into contributions from different electronic states (certain bands or energy regions) or angular momenta (p, d contributions of the wave functions to the anisotropy of the charge density as discussed for example in Schwarz et al.[4] for the high-temperature superconductor $YBa_2Cu_3O_7$).

(18) Herzog, P.; Freitag, K.; Reuschenbach, M.; Walitzki, H. *Z. Phys. A* **1980**, *294*, 13.
(19) Schwarz, K.; Blaha, P. *Lecture Notes Chem.* **1998**, *67*, 139.
(20) Blaha, P.; Schwarz, K.; Luitz, J. *WIEN97*; Vienna University of Technology: Vienna, 1997. (Improved and updated UNIX version of the original WIEN code published by Blaha, P.; Schwarz, K.; Sorantin, P.; Trickey, S. B.; *Comput. Phys. Commun.* **1990**, *59*, 399.)
(21) Perdew, J. P.; Chevary, J. A.; Vosko, S. H.; Jackson, K. A.; Pederson, M. R.; Singh, D. J.; Fiolhais, C. *Phys. Rev.* **1992**, *B46*, 6671.
(22) Perdew, J. P.; Wang, Y. *Phys. Rev.* **1992**, *B45*, 13244.
(23) Kohler, B.; Wilke, S.; Scheffler M.; Kouba, R.; Ambrosch-Draxl, C. *Comp. Phys. Commun.* **1996**, *94*, 31.

Table 1. Crystal Data and Refinement Results for $Cd(OH)_2$[a]

space group	$P\bar{3}m1$
a (Å)	3.49494(3)
b (Å)	3.49494(3)
c (Å)	4.7059(1)
V (Å^3)	49.780(2)
Z	1
calcd density (g/cm^3)	4.8838(2)
abs coeff (cm^{-1})	878.35
F(000)	66
radiation	Cu Kα_1 (λ = 1.540 51 Å)
$2\theta_{max}$ (deg)	92
no. of peaks	19
mode of refinement	full profile
scale factor	0.6142(1)
texture parameter and axis	1.065(4) [001]
temperature (°C)	21
R (intensity)[b]	0.041
R (profile)[c]	0.078
B_{iso} (Å^2) Cd	1.05(1)
B_{iso} (Å^2) O	1.52(1)
B_{iso} (Å^2) H	1.8[d]

[a] Numbers in parentheses are standard deviations. Previous structure determinations have given $a = b = 3.496$ Å, $c = 4.702$ Å[1,2]. [b] $R(\text{intensity}) = \sum(|I_{obs} - I_{calc}|)/\sum I_{obs}$. [c] $R(\text{profile}) = \sum(|Y_{obs} - Y_{calc}|)/\sum Y_{obs}$. [d] Fixed at $1.2B_{iso}$ for the oxygen atom. The z(O) and z(H) values are given in Table 3.

Table 2. X-ray Diffraction Data of $Cd(OH)_2$ from Full Profile Refinements

h	k	l	d (Å)	θ (deg)	I_{obs}	I_{calc}
0	0	1	4.70593	18.841	9813	10000
0	1	0	3.02671	29.486	6495	6717
0	1	−1	2.54564	35.225	3107	3211
0	1	1	2.54564	35.225	8898	9197
0	0	2	2.35297	38.217	891	859
0	1	−2	1.85766	48.993	2314	2474
0	1	2	1.85766	48.993	2638	2820
1	1	0	1.74747	52.308	2654	2720
1	1	1	1.63817	56.094	2629	2768
0	0	3	1.56864	58.817	367	323
0	2	0	1.51335	61.191	758	778
0	2	−1	1.44069	64.640	1134	1161
0	2	1	1.44069	64.640	522	535
1	1	2	1.40290	66.603	873	965
0	1	−3	1.39271	67.155	959	1038
0	1	3	1.39271	67.155	520	563
0	2	−2	1.27282	74.480	611	648
0	2	2	1.27282	74.480	543	576
0	0	4	1.17648	81.796	183	171
1	1	3	1.16732	82.577	583	647
1	2	0	1.14399	84.646	586	565
1	2	−1	1.11161	87.723	442	439
1	2	1	1.11161	87.723	838	831
0	1	−4	1.09656	89.245	273	301
0	1	4	1.09656	89.245	194	215
0	2	−3	1.08913	90.019	212	236
0	2	3	1.08913	90.019	360	401

Results

Structure Determination. The crystals prepared as described were small plates. Freshly precipitated crystals showed no sign of contamination with $CdCO_3$ as judged by X-ray diffraction. However, the crystals slowly accumulated carbonate, and aged crystals (several weeks old) stored in air showed a clear presence of $CdCO_3$ as judged by X-ray diffraction.

The results of the full profile analysis is given in Tables 1 and 2 and Figure 2. The profile parameters include half-width, asymmetry, zero shift, pseudo-Voigt, half-width anisotropy, and

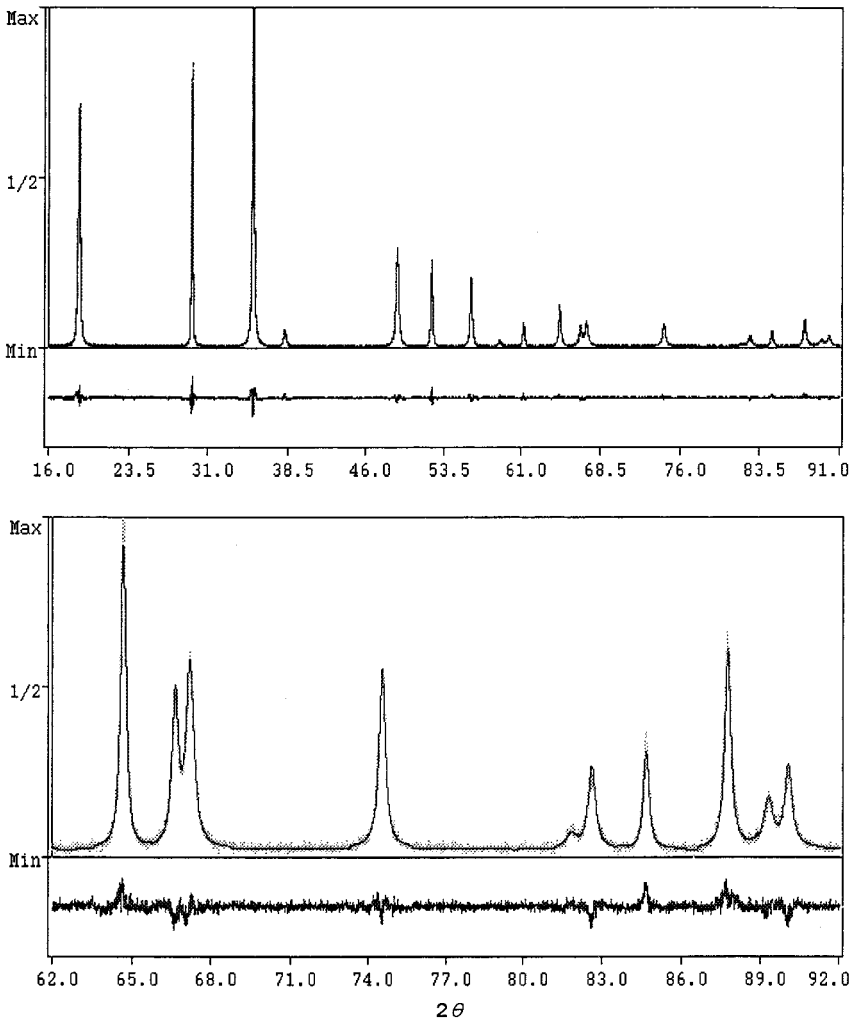

Figure 2. X-ray diffraction pattern of $Cd(OH)_2$. Observed, calculated (full line), and difference intensities are plotted vs 2Θ. The top diagram shows the 19 peaks included in the full profile analysis. The half-width anisotropy is noticeable. The bottom diagram is a magnification of the last part of the top diagram.

Table 3. Free Structural Parameters of $Cd(OH)_2$ Determined by X-ray Diffraction and LAPW Calculations[a]

	X-ray diffraction		LAPW	
atom	this work *z*/*c*	BD70 *z*/*c*	LDA *z*/*c*	GGA *z*/*c*
0	0.2307(10)	0.241(9)	0.2312	0.2388
H	0.420(5)	–	0.4400	0.4457

[a] Numbers given in parentheses are standard deviations. BD70 refers to ref 2.

pseudo-Voigt anisotropy. Inspection of the half-widths revealed that especially the 001 peaks showed pronounced broadening, which could be interpreted as the sample consisting of thin crystal plates with the *c* axis perpendicular to the plate plane. This was confirmed by inclusion of a texture parameter with a 001 axis.

Refinements based on intensities, instead of the full profile, resulted in the same atomic parameters, within the standard deviation, as those obtained by the full profile analysis.

The cell parameters are in agreement with what has been obtained in earlier investigations[1,2] and so is the z-parameter of the oxygen atom (see Table 3).

We also performed a series of LAPW calculations using the WIEN97 code.[20] The *z* position of the O and H atoms in $Cd(OH)_2$ in the crystalline state was optimized both at the LDA and GGA level of theory, see Table 3. There is good agreement between the X-ray diffraction and LAPW results, except for a slightly smaller *z*(H) from X-ray data compared to the calculations.

The positions of the H atoms may not be well defined from X-ray diffraction because this technique determines the electron density rather than the position of the nuclei. This has a drawback when comparing with quantum chemical calculations, in which the positions of the nuclei directly enter the Hamiltonian. No other studies have been made for the position of the hydrogen nucleus in $Cd(OH)_2$, but for $Ca(OH)_2$ detailed studies have been performed using both X-ray and neutron diffraction to determine the position of the hydrogen nucleus.[24,25] For this isostructural compound the O−H distance found by X-rays diffraction was 0.79 Å, while neutron diffraction gave a much more reliable value of 0.93 Å. In addition the free OH^- ion bond length is[26,27] 0.96 Å, supporting the value found in the LAPW calculations in this work.

Figure 1 shows the hexagonal unit cell, in which one cadmium ion is surrounded by six oxygens. Table 4 gives some important distances and angles in the crystal structure.

(24) Petch, H. E. *Acta Crystallogr.* **1961**, *14*, 950.
(25) Busing, W. R.; Levy, H. A. *J. Chem. Phys.* **1957**, *26*, 563.
(26) Owrutsky, J. C.; Rosenbaum, N. H.; Tack, L. M.; Saykally, R. J. *J. Chem. Phys.* **1985**, *83*, 5338.
(27) Lee, T. J.; Dateo, C. E. *J. Chem. Phys.* **1997**, *107*, 10373.

Table 4. Distances (Å) and Angles (deg) in the Crystal Structure[a]

			LAPW			
	X-ray diff.		LDA		GGA	
bond or angle	distance	angle	distance	angle	distance	angle
Cd−O1	2.291		2.294		2.311	
O1−H1	0.891		0.982		0.972	
O2−H1	2.603		2.544		2.506	
O1−02	3.240		3.236		3.180	
O1−02″	2.964		2.967		3.020	
O1−H1−O2		129.2		127.6		126.3
O1−Cd−O2″		80.6		80.5		81.6
O1−Cd−O1′		99.4		99.5		98.4

[a] Symmetry code: ′ corresponds to a (x, $y - 1$, z) translation; ″ corresponds to a (x, y, $z - 1$) translation.

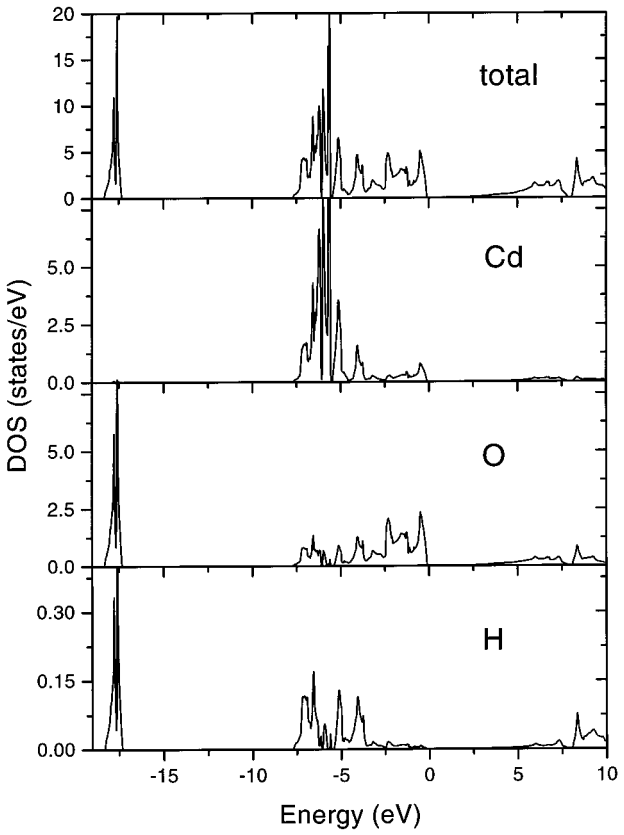

Figure 3. Density of states (DOS) as a function of energy. The total DOS is decomposed into site-projected contributions from one Cd, O, and H atomic sphere (note the different scales for Cd, O, and H). The DOS corresponding to the charge in the interstital region is not shown here.

Chemical Bonding. In this section we discuss the results from our LAPW calculations and their interpretation in terms of chemical bonding. The total and site projected DOS are presented in Figure 3. The lowest band at about −18 eV originates from O 2s (2p) and H 1s states. The Cd 4d states form the main contribution in the energy range −8 to −4 eV ("d" band) but they show an admixture from some of the O 2p bands and have a significant dispersion so that a purely ionic picture is definitely too simple. The highest occupied bands (between −4 and 0 eV) originate mainly from O 2p states and thus we denote this energy region as "p" band. A gap of about 1.5 eV separates these highest occupied from the lowest unoccupied states, which have predominantly Cd 5s,5p character. (It is well known that the gap is not a ground state property and thus in density functional theory based calculations it often has only half the experimental value.)

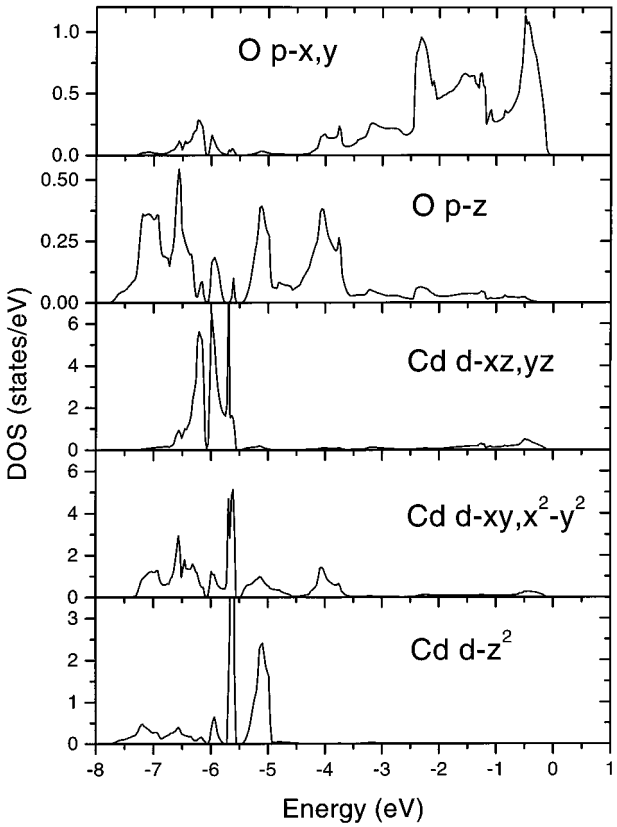

Figure 4. Decomposition of the site-projected DOS into symmetry decomposed O p and Cd d contributions.

The crude picture of the chemical bonding is best described as Cd^{2+} and OH^- ions bound together by ionic interactions. The molecular orbital of the latter ion is determined by a covalent bond between H and an sp hybrid orbital involving the O p_z. The other two O 2p orbitals, O p_x and O p_y, remain at their (about 4 eV) higher energy, a feature which is already present in a free OH^- ion, where these states are separated by a similar amount according to our RHF/6-31G(d)[28−30] calculation using Gaussian94.[31]

In Figure 4 the O 2p and Cd 4d DOS within the "d" and "p" band is further decomposed into their respective components (i.e., irreducible representations). A clear separation of the O p_z and $p_{x,y}$ states by about 4 eV is evident similar to the free OH^- ion. Nevertheless the Cd 4d states dominate the low-energy region of the DOS (note the different normalization of the partial O p and Cd d DOS!) but show—due to polarization by O—quite a considerable energy dispersion. The d_{z^2} orbitals have the weakest interaction with O and consequently show the strongest localization. The d_{xy}, $d_{x^2-y^2}$ (and to a smaller extent the d_{xz}, d_{yz}) orbitals point close to the O atoms and thus contribute to the DOS even near the top of the valence band.

(28) Hehre, W. J.; Ditchfield, R.; Pople, J. A. *J. Chem. Phys.* **1972**, *56*, 2257.
(29) Hariharan, P. C.; Pople, J. A. *Chem. Phys. Lett.* **1972**, *66*, 217.
(30) Francl, M. M.; Pietro, W. J.; Hehre, W. J.; Binkley, J. S.; Gordon, M. S.; Defrees, D. J.; Pople, J. A. *J. Chem. Phys.* **1982**, *77*, 3654.
(31) Frisch, A. M.; Trucks, G. W.; Schlegel, H. B.; Gill, P. M. W.; Johnson, B. G.; Robb, M. A.; Cheeseman, J. R.; Kieth, G. A.; Petersson, G. A.; Montgomery, J. A.; Raghavachari, K.; Al-Laham, M. A.; Zakrzewski, V. G.; Ortiz, J. V.; Foresman, J. B.; Cioslowski, J.; Stefanov, B.; Nanayakkara, A.; Challacombe, M.; Peng, C. Y.; Ayala, P. Y.; Chen, W.; Wong, M. W.; Andres, J. L.; Replogle, E. S.; Gomperts, R.; Martin, R. L.; Fox, D. J.; Binkley, J. S.; Defrees, D. J.; Baker, J.; Stewart, J. J. P.; Head-Gordon, M.; Gonzales, C.; Pople, J. A. *Gaussian 94*, Revision D.1 and D.4; Gaussian, Inc.: Pittsburgh, PA, 1995.

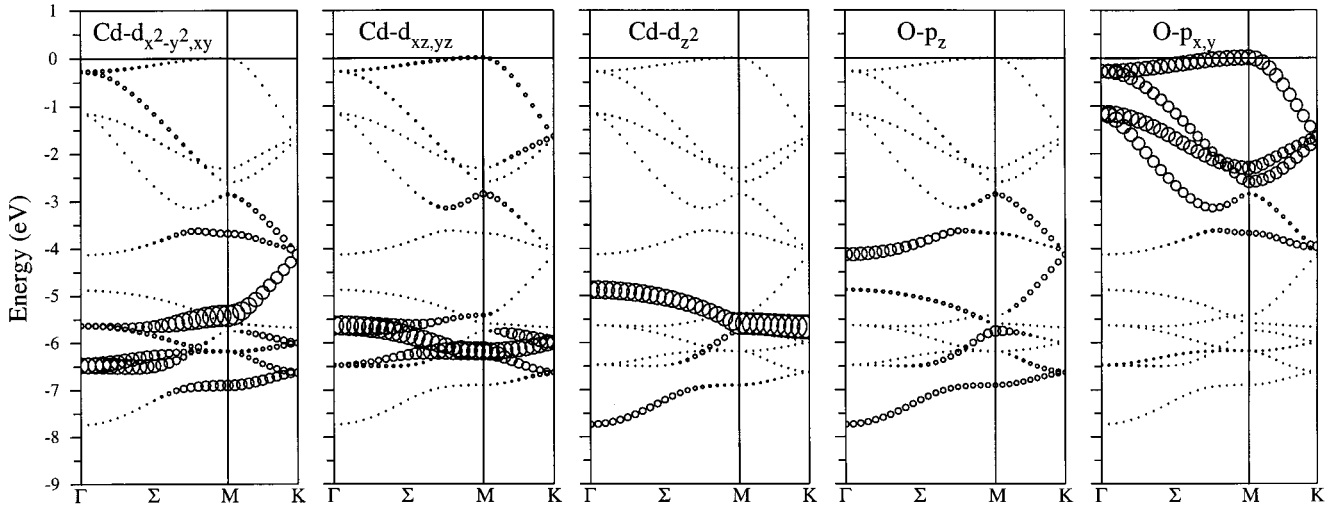

Figure 5. Band structure of Cd(OH)$_2$. The radius of the circles is proportional to the respective partial charge of the given state.

This interaction between the O p and Cd d states can also be seen in the energy band structures displayed in Figure 5, where the character of each state E_{nk} is represented by a circle with a radius that is proportional to the respective partial charges of the component indicated at the top of the panel. In particular at higher energies the d_{xy},$d_{x^2-y^2}$ and d_{xz},d_{yz} admixture is visible in the predominantly O $p_{x,y}$ bands and at low energy the O p_z admixture to the Cd 4d bands is aparent. These interactions would increase or decrease with respect to the z(O) parameter, which is determined by finding an optimal balance.

Electric Field Gradient. From the PAC experiment the experimental and fitted $A_2G_2(t)$ as well as their Fourier transforms (giving the three frequencies in eq 2) are shown in Figure 6. The fitted parameters and the derived V_{zz} are given in Table 5. The first 449.6 ns (400 points) of the spectrum were used in the fit, except for the first 3 points for which there are systematic errors. The uncertainty on V_{zz} was estimated from eq 4, using conventional propagation of errors. The major contribution comes from the uncertainty on the nuclear quadrupole moment, Q. Only one metal coordination geometry is found, as expected, and η is almost zero, indicating a structure in which the EFG has (almost) axial symmetry. This is in good agreement with the structure determined by X-ray diffraction, according to which the z axis is a 3-fold symmetry axis (Figure 1) and thus (according to symmetry) the asymmetry in the EFG should exactly be zero. Small differences in coordination geometry may occur from cadmium to cadmium nucleus, but inclusion of such effects (described by a Gaussian distribution centered at ω_0) did not significantly change the χ^2 of the fit, nor did an inclusion of a rotational diffusion.[32] This behavior is expected for a crystalline sample, and consequently these effects were not included in the fit presented here.

The EFG was calculated using the LAPW method at both, the LDA and GGA equilibrium geometries, as well as at slightly different Cd−OH and O−H bond lengths (keeping the other distance fixed) in order to investigate the influence of these parameters on the EFG (Figure 7).

The EFG at the oxygen and hydrogen nuclei are presented. Although experimental data are presently not available for Cd(OH)$_2$, data for several alkali and earth alkali hydroxides do exist.[33] From Figure 7 we see that the O and H EFG do not depend much on the distance of the OH group from the Cd plane, but they obviously are sensitive to the O−H distance. The EFG at the theoretical LDA minimum corresponds to a nuclear quadrupole coupling constant of 0.27 and 6.5 MHz for D and ^{17}O, respectively. Both of these values fall in the range of the data measured for the other hydroxides. The O−H

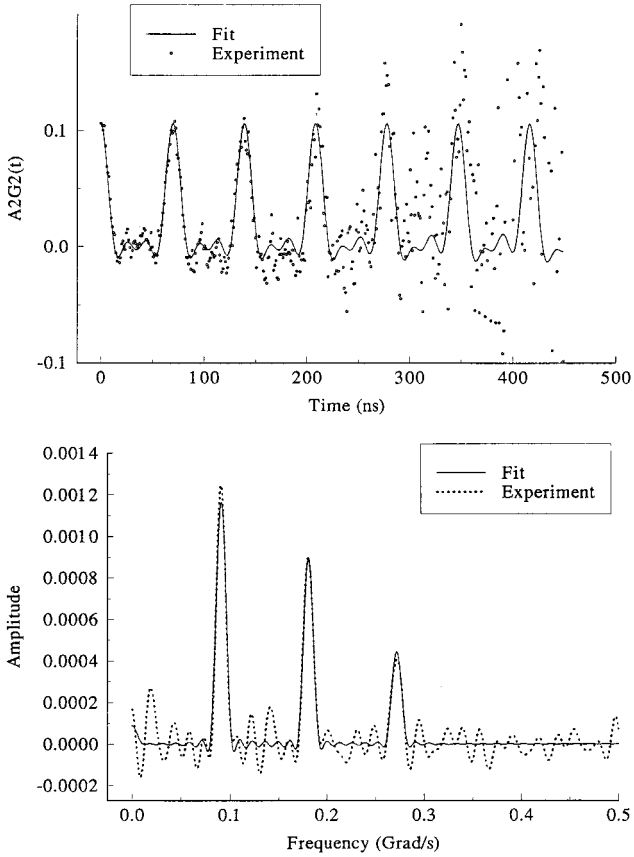

Figure 6. PAC spectrum and fit (upper panel) and Fourier transforms of these (lower panel).

Table 5. Parameters Fitted to the PAC Experiment[a]

ω_0	90.5 ± 0.1 Mrad/s
η	0.06 ± 0.02
V_{zz}	$(\pm 4.92 \pm 0.75) \times 10^{21}$ V/m^2

[a] ω_0 and η were fitted and V_{zz} was derived according to eq 4. The sign of V_{zz}, cannot be determined by ^{111m}Cd PAC.

(32) Danielsen, E.; Bauer, R.; Schneider, D. *Eur. J. Biophys.* **1991**, *20*, 193.
(33) Poplett, I. J. F. *J. Magn. Reson.* **1982**, *50*, 382.

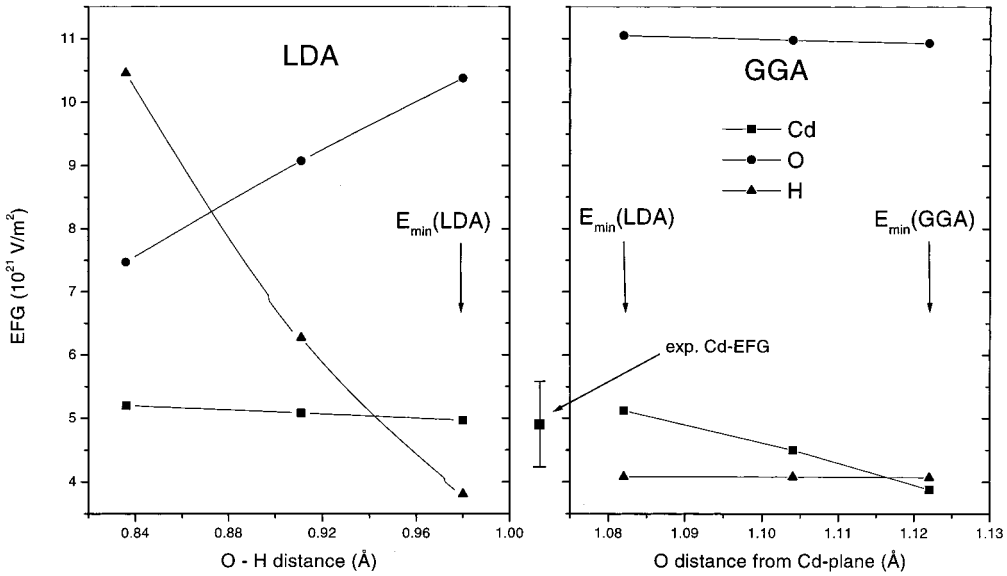

Figure 7. Theoretical EFG of Cd, O, and H for different structural parameters. (left panel, calculated within LDA): EFG for different O−H distances. (Right panel, calculated within GGA): EFG for different z(O) values (the O distance from the plane of cadmium ions (see Fig. 1) corresponds to z(O)). (■) Cd, (●) O, (▲) H. The experimental Cd EFG ($(\pm 4.92 \pm 0.75) \times 10^{21}$ V/m^2) is given as an interval corresponding the one standard deviation. The equilibrium positions within LDA or GGA are marked by arrows.

Table 6. Decomposition of the Theoretical Cd-EGF (10^{21} V/m^2)[a]

energy region	V^{p}_{zz}	V^{d}_{zz}	$V^{tot}zz$
≈ −60 eV	−0.44*	−	−0.44
≈ −18 eV	+0.58	+0.10	+0.69
−8 to −4 eV	+4.50	−18.27	−13.77
−4 to 0 eV	−1.50	+20.00	+18.50
total	+3.14	+1.84	+4.98
experiment	−	−	±4.92

[a] At the LDA equilibrium structure into contributions from different energy regions (rows) and from contributions of wavefunctions corresponding to different angular momenta (columns), i.e., Cd 5p (* 4p) or 4d labeled V^{p}_{zz} and V^{d}_{zz}, respectively. The four energy regions correspond to the "Cd 4p", "O 2s and H 1s", "Cd 4d", and the "O 2p" bands, respectively (see section on chemical bonding).

distance determined by X-ray diffraction would lead, e.g., to a 50% larger H EFG in contrast to literature. The EFG of the free OH^- ion has been calculated by Sundholm et al.[34] and is 4.69×10^{21} V/m^2 and 16.2×10^{21} V/m^2 for H and O, respectively (with an O−H bond length of 0.97 Å). These results compare well for the EFG at the hydrogen nucleus (see Figure 7) but the calculated EFG at the oxygen nucleus is about 50% lower than in the present crystal, indicating significant differences between OH^- in the gas phase and in the crystal.

As expected the O−H distance has little influence on the Cd EFG, whereas the value of z(O) has. At the LDA equilibrium position an EFG of about 4.98×10^{21} V/m^2 was obtained in perfect agreement with experiment, while at the GGA equilibrium the resulting EFG is smaller by 20% (3.88×10^{21} V/m^2). The EFG tensor is axially symmetric ($\eta = 0$) for the assumed crystal symmetry. Spin−orbit effects turned out to be negligible (about +1%, i.e., much less than the precision of the calculation). The origin of the EFG has been analyzed and the results are presented in Table 6. The contributions of the low-lying Cd 4p and O 2s states are small and almost cancel each other. The Cd d band contributions (defined as those states at the bottom of the valence band containing 10 electrons) and the O p band (top of the valence band containing 12 electrons) have both very large contributions which partially cancel each other.

The EFG is caused by the anisotropy of the charge distribution around the nucleus in question. As shown previously,[4] the main contributions can arise from p- and d-like wavefunctions of the corresponding atom and this will be discussed below. Quite unexpectedly, the Cd 4d states contribute significantly to the EFG due to the strong polarization by O as illustrated above in the partial DOS. Although these states are fully occupied, they are spread over a wide energy range (see Figure 4) with varying radial wavefunctions and thus have different $\langle r^{-3} \rangle$ expectation values causing a large EFG. The main contribution to the EFG still comes from the asymmetry of Cd 5p electrons (Table 6). However, one might interprete these contributions mainly as orthogonalized tails from the O 2p wavefunctions, which enter the Cd sphere and thus must be reexpanded at the Cd site according to the LAPW method.

Discussion

The overall agreement between the structure as determined from X-ray diffraction or LAPW total energy minimization is quite reasonable. Additional support for the value of z(H) comes from neutron diffraction on $Ca(OH)_2$, which has an O−H bond length similar to what is found in this work. The technique of neutron diffraction is not practical for $Cd(OH)_2$ due to the high cross-section of naturally occurring cadmium for neutrons. Somewhat unexpectedly the GGA equilibrium structure differs more from experiment than the LDA results. GGA yields a larger Cd-O distance and this also influences the Cd-EFG significantly. Again, the LDA structure gives an EFG in better agreement with experiment, but due to the uncertainty in the nuclear quadrupole moment of ^{111}Cd (in the $I = {}^5/_2$ state) the EFG derived from the PAC experiment has an overall uncertainty of about 15%. This almost brings the EFG calculated at the GGA level within the uncertainty of the experimentally determined EFG. Changes of the EFG when changing the z(O) position are significant (about 0.27×10^{21} V/m^2 for a change of 0.01 Å). The PAC experiments show that the assymetry parameter η might differ slightly from zero. This would for instance require a small tilting of the OH^- ion with respect to the z axis, or could be caused by vibrations of this type (tilting).

(34) Sundholm, D.; Pyykkö, P.; Laaksonen, L. *Mol. Phys.* **1985**, *56*, 1411.

The chemical bonding is primarily ionic and one can even recognice the electronic levels of a free OH^- ion in the crystalline DOS. However, the 4d states of Cd are strongly polarized by the OH^- ions and this cannot be neglected in the description of the interaction. This clearly shows up when analyzing the origin of the EFG, where about $^1/_3$ of the total EFG comes from the polarized Cd 4d states (V_{zz}^{d}). The remaining $^2/_3$ come from Cd 5p electrons (V_{zz}^{p}), but this might be better interpreted as an effect of expanding the tails of the O 2p wavefunctions (extending into the cadmium sphere) into cadmium basis functions.

Acknowledgment. This work was partly supported by the Hochschuljubiläumsstiftung der Stadt Wien and by the Danish Natural Science Research Council via the Center for Bioinorganic Chemistry.

IC990018E